ELSEVIER

Water Research 38 (2004) 1715–1732

WATER RESEARCH

www.elsevier.com/locate/watres

Application of multiway ICA for on-line process monitoring of a sequencing batch reactor

Chang Kyoo Yoo*, Dae Sung Lee, Peter. A. Vanrolleghem

BIOMATH, Department of Applied Mathematics, Biometrics and Process Control, Ghent University, Coupure Links 653, B-9000 Gent, Belgium

Received 6 May 2003; received in revised form 17 December 2003; accepted 7 January 2004

Abstract

Multiway principal component analysis has been shown to be a powerful monitoring tool in many industrial batch processes. However, it has the shortcomings that all batch lengths should be equal, the measurement variables must be normally distributed and that future values of the current batch must be estimated to allow on-line monitoring. In this work, it is shown that multiway independent component analysis (MICA) can be used to overcome these drawbacks and obtain better monitoring performance. The on-line MICA monitoring of batch processes is based on a new unfolding method and independent component analysis (ICA). ICA provides better monitoring performance than PCA in cases with non-Gaussian data because it is not based on the assumption that the latent variables are normally distributed. The MICA algorithm does not require any estimation of future batch values and can also be applied to non-equal batch length data sets. This article describes the application of on-line MICA monitoring of a sequencing batch reactor (SBR). It is successfully applied to an 80L SBR for biological wastewater treatment, which is characterized by a variety of disturbance sources with non-Gaussian characteristics. The SBR poses an interesting challenge from the point of process monitoring characterized by non-stationary, batchwise, multiscale, and non-Gaussian characteristics. The results of the bench-scale SBR monitoring clearly showed the power and advantages of MICA monitoring in comparison to conventional monitoring methods.

Keywords: Batch monitoring; Biological wastewater treatment; Multiway independent component analysis (MICA); On-line process monitoring; Sequencing batch reactor (SBR)

1. Introduction

Sequencing batch reactor (SBR) processes have demonstrated their efficiency and flexibility in the treatment of wastewaters with high concentrations of nutrient, nitrogen, phosphorous, and toxic compounds from domestic and industrial sources. SBRs have a unique cyclic batch operation, usually with five well-defined phases: fill, react, settle, draw and idle. Most of the advantages of SBR processes may be attributed to their single-tank designs and the flexibility allowing them to meet many different treatment objectives, which derives from the possibility of adjusting the duration of the different phases. Real-time control of the SBR process can contribute to this. A possible control strategy is based on the identification of the endpoint of a biological reaction. Switching to the next phase shortly after the detection of the reaction endpoint provides an optimum solution for both the process performance and the economics of the plant. In fact, if the duration of a phase is too short, the removal of the pollutants is not complete and the quality of the effluent will not meet the limits imposed by law. On the other hand, cycles which are longer than necessary decrease the capacity of the plant (volume of wastewater treated

*Corresponding author. Tel.: +32-9264-5935; fax: +32-9264-6220.

E-mail address: changkyoo.yoo@biomath.ugent.be (C.K. Yoo).

0043-1354/$ - see front matter © 2004 Elsevier Ltd. All rights reserved.
doi:10.1016/j.watres.2004.01.006

Nomenclature

$\mathbf{A}$	mixing matrix
a	the number of latent variables in PCA
$\mathbf{B}$	separating matrix for whitened vector $\boldsymbol{z}$
$\mathbf{B}_d$	deterministic part of $\mathbf{B}$
$\mathbf{B}_e$	excluded part of $\mathbf{B}$
d	the number of variables
E	expectation operator
$\mathbf{E}$	residual matrix
$\mathbf{e}(k)$	kth row of $\mathbf{E}$
$\mathbf{I}_{ICA}$	the score matrix of MICA
I^2	I^2 statistic for MICA monitoring
I_e^2	I_e^2 statistic for MICA monitoring
m	the number of latent variables in MICA
n	the number of samples
k	time index
$\mathbf{P}$	loading matrix
$\mathbf{Q}$	whitening matrix
$\mathbf{S}$	independent component matrix
$\mathbf{S}_d$	deterministic part of $\mathbf{S}$
$\mathbf{S}_e$	excluded part of $\mathbf{S}$
$\mathbf{s}(k)$	the kth column vector of $\mathbf{S}$
$\mathbf{s}_e(k)$	the kth column vector of $\mathbf{S}_e$
SPE	squared prediction error
$\mathbf{T}$	score matrix
T^2	Hotelling's T^2 statistic
$\mathbf{U}$	orthogonal matrix generated from the eigen-decomposition of $\mathbf{R}_x$
$\mathbf{W}$	separating matrix for original data vector $\mathbf{x}$
$\mathbf{W}_d$	deterministic part of $\mathbf{W}$
$\mathbf{W}_e$	excluded part of $\mathbf{W}$
$\mathbf{X}$	data matrix ($\mathbf{X}\in R^{n\times d}$ in PCA, $\mathbf{X}\in R^{d\times n}$ in ICA)
$\mathbf{x}$	d-dimensional column vector of data matrix
$x_j(k)$	the entry in the jth row and kth column of $\mathbf{X}$
$\hat{\mathbf{x}}$	predicted data vector
$\mathbf{z}$	whitened data vector

per day) or increase its operating costs; an aerobic phase which is too long would also mean wasting energy for aeration [1,2].

The SBR process is highly nonlinear, time varying and subject to significant disturbances like hydraulic changes, composition variations and equipment failures. Small changes in concentrations or flows may effect effluent quality and microorganism growth. Moreover, compared to continuous wastewater treatment processes, SBR operation data have the added dimension of batch number, in addition to the measured variables and sample times (batches × variables × time), that is, a three-way matrix. Batch processes generally exhibit some batch-to-batch variation in the trajectories of the process variables. Normal variation is due to typical variations in the operation whereas special variations are due to exceptional phenomena [3]. However, treatment performance, the key indicator of process performance, is often examined off-line in a laboratory. Even though operators are aware that there are some problems in treatment performance, they cannot quickly find out or deduct what the causes are and predict when they will occur because most batch processes are run without any effective form of on-line monitoring. Therefore, on-line monitoring and fault diagnosis of batch processes are crucial to detect faults that can be corrected prior to completion of the batch or can be corrected in subsequent batches. Early detection of problems and correction of deviations by on-line monitoring before the completion of the batch can save the batch and reduce the number of rejected batches.

Several techniques using multivariate statistical analysis have been developed for on-line monitoring and fault detection of batch processes. Nomikos and Macgregor [5,6] have extended the multivariate statistical process control (SPC) methods of Principal Component Analysis (PCA) to batch processes, where the method is called multiway PCA (MPCA). The key idea of MPCA is to compress the normal batch data and extract the important information by projecting the data onto a low-dimensional space that summarizes both the variables and their time trajectories. The progress of a new batch is then monitored by comparing the progresses of the projections in the reduced space with those collected from normal batch data. Dong and McAvoy [4] used nonlinear principal component analysis (NLPCA) based on principal curves and neural networks to monitor batch processes. Rännar et al. [7] suggested an adaptive batch monitoring method using hierarchical PCA to overcome the need of estimating the missing data on trajectory deviation from the current time until the end of the batch in PCA. There are many papers related to the application of MPCA to industrial batch monitoring [8–18].

MPCA has a fundamental shortcoming as it assumes equal batch lengths and a Gaussian distribution of the variables. Moreover, the necessity to predict the future values of a batch in MPCA might cause false detection because the predicted values that do not consider a dynamic relationship may distort the data information. To solve these problems, we will apply an on-line monitoring method, called multiway independent component analysis (MICA), to the SBR process. It uses a simple unfolding method and applies the independent component analysis [19,20].

This paper is organized as follows. The MPCA and the MICA monitoring are introduced in the next section. Then the on-line monitoring procedure of MICA is

explained. The results of a bench scale SBR plant are then given to illustrate the power and advantages of the MICA monitoring in comparison to MPCA. Finally, conclusions are given.

2. MPCA

MPCA is used for analysis and monitoring of batch process data. The batch data are reported in terms of batch runs, variables and times. Data are arranged into a three-dimensional (3-D) matrix $\underline{\mathbf{X}}(I \times J \times K)$, where I is the number of batches, J is the number of variables and K is the number of sampling times in a given batch. It can be decomposed using various three-way techniques, including MPCA. Multiway PCA is equivalent to performing an ordinary PCA on a large 2-D matrix $\mathbf{X}$ constructed by unfolding the three-way data as shown in approach of Fig. 1 [4].

MPCA decomposes the three-way $\underline{\mathbf{X}}$ array into a summation of the product of the score vector t_r and the loading matrix P_r plus the residual array $\underline{\mathbf{E}}$ that is minimized in least-squares sense as

$$\underline{\mathbf{X}} = \sum_{r=1}^{R} t_r \otimes P_r + \underline{\mathbf{E}} = \sum_{r=1}^{R} t_r p_r^{\mathrm{T}} + \mathbf{E} = \hat{\mathbf{X}} + \mathbf{E}, \tag{1}$$

where $\otimes$ denotes the Kronecker product ($\underline{\mathbf{X}} = \mathbf{t} \otimes \mathbf{P}$ is $\underline{X}(i,j,k) = t(i)P(j,k)$) and R denotes the number of principal components retained. The first equation in Eq. (1) denotes the 3-D decomposition while the second equation displays the more common 2-D decomposition.

The statistics used for a MPCA are Hotelling's T^2 and squared prediction error (SPE). If a new batch is good and consistent with the normal batches, its scores should fall within the normal range and the SPE or Q-statistic should be small. The T^2 and Q-statistics obtained at end-of-batch for batch i are calculated as

$$T_i^2 = \mathbf{t}_{\mathrm{new}}^{\mathrm{T}} \mathbf{S}^{-1} \mathbf{t}_{\mathrm{new}} \sim \frac{R(I^2-1)}{I(I-R)} F_{R,I-R}, \tag{2}$$

$$Q_i = \mathbf{e}_i \mathbf{e}_i^{\mathrm{T}} = \sum_{c=1}^{KJ} \mathbf{E}(i,c)^2, \tag{3}$$

where $\mathbf{e}_i$ is the ith row of $\mathbf{E}$, I is the number of batches in the reference set, $\mathbf{t}_r$ is a vector of R scores, $\mathbf{S}$ is the $(R \times R)$ covariance matrix of the t-scores calculated during the model development (diagonal due to the orthogonality of the t score values), R is the number of principal components retained in the model, $F_{R,I-R}$ is the F-distribution value with R and $I-R-1$ degrees of freedom. Statistical limits on the T^2 and Q-statistics are computed by assuming that the data have a multivariate normal distribution [21].

Wold [22] used another unfolding approach (approach B in Fig. 1) for modeling and diagnosis of batch processes. This approach does not have the constraint that the batch length should be equal and future-missing values should be estimated. However, the mean centering of the unfolding matrix required by this approach cannot remove the batch process trajectory since it is based on the batch monitoring around the mean of the variables during all batches.

Two problems can arise with the MPCA method of Nomikos and MacGregor's approach when used for

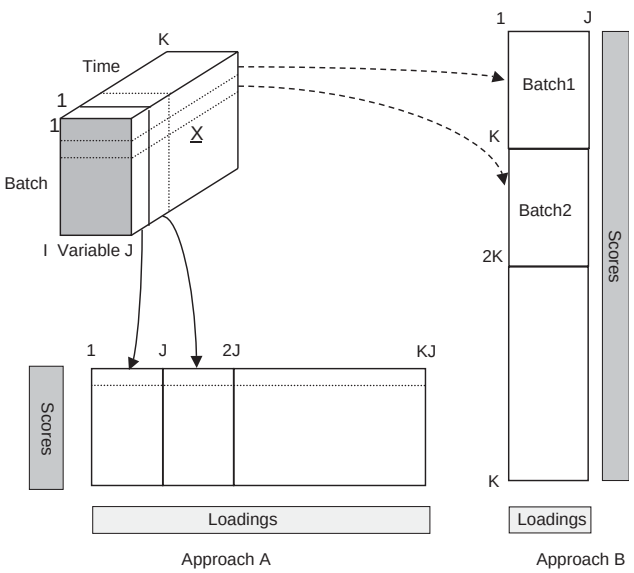

Fig. 1. Two unfolding methods. Approach A: unfolding timewise [5] and approach B: unfolding batchwise [22].

on-line batch monitoring: the occurrence of an incomplete data matrix and unequal batch length. The first major problem arises when the monitoring is performed at a time instant where the data matrix is not complete yet. Nomikos and MacGregor [5] suggested three different ways for variable trajectory estimation, i.e. to complete the remaining of the batches: (1) zero deviation, (2) current deviation and (3) PCA projection method. The second problem of MPCA is that that the length of the modeled batches should be the same. There are many situations in which the total duration of the batches or the duration of various phases (stages) within the batches is not the same. To handle these problems simply, another unfolding method has to be developed.

3. MICA batch monitoring

The fault detection method, which monitors the process operation, is related to hidden information latent in the multidimensional data. So, a key point is how to extract the hidden information from the multidimensional data set. In this paper, we adopt the independent component analysis (ICA) technique. In ICA, the latent variables are allowed to be non-Gaussian and mutually independent. ICA seeks to extract these independent components as well as the so-called mixing process among them [19,23–26].

3.1. Independent component analysis (ICA)

To introduce the ICA algorithm, it is assumed that d measured variables, $\mathbf{x}(k) = [x_1(k), \ldots, x_d(k)]^{\mathrm{T}}$ at sample k can be expressed as linear combinations of m ($\leqslant d$) unknown independent components $s_1, s_2, \ldots, s_m$:

$$\mathbf{x}(k) = \sum_{j=1}^{m} \mathbf{a}_j \mathrm{s}_j(k) = \mathbf{A}\mathbf{s}(k), \tag{4}$$

where $\mathbf{x}(k)$ is linearly mixed with m components of $\mathrm{s}_j(k)$. The independent components and the measured variables have zero means. The relationship between them is given by

$$\mathbf{X} = \mathbf{A}\mathbf{S} + \mathbf{E}, \tag{5}$$

where $\mathbf{X} = [\mathbf{x}(1), \mathbf{x}(2), \ldots, \mathbf{x}(n)] \in R^{d\times n}$ is the data matrix, $\mathbf{A} = [\mathbf{a}_1, \ldots, \mathbf{a}_m] \in R^{d\times m}$ is the mixing matrix, $\mathbf{S} = [\mathbf{s}(1), \mathbf{s}(2), \ldots, \mathbf{s}(n)] \in R^{m\times n}$ is the independent component matrix, $\mathbf{E} \in R^{d\times n}$ is the residual matrix, and n is the number of samples. The basic problem of ICA is to estimate the original components $\mathbf{S}$ or to estimate $\mathbf{A}$ from $\mathbf{X}$ without any knowledge of $\mathbf{S}$ or $\mathbf{A}$. Therefore, the objective of ICA is to calculate a separating matrix $\mathbf{W}$ so that the components of the reconstructed data matrix $\mathbf{S}$, given as

$$\hat{\mathbf{S}} = \mathbf{W}\mathbf{X} \tag{6}$$

become as independent of each other as possible. Using the ICA algorithm, we can obtain the rows of $\mathbf{S}$ whose norm is 1. Compared to the PCA, the $\mathbf{S}$ and $\mathbf{W}$ matrix in Eq. (6) may be considered as a loading matrix and a score matrix, i.e. $\mathbf{S}$ can be regarded as the score matrix $\mathbf{T}$, while $\mathbf{W}$ can be treated as loading matrix $\mathbf{P}$ [25,27].

The initial step in ICA is whitening, also known as *sphering*, which eliminates all the cross-correlation between random variables. Consider a d-dimensional random vector $\mathbf{x}(k)$ at sample k with covariance $\mathbf{R}_{\mathbf{x}} = E(\mathbf{x}(k)\mathbf{x}^{\mathrm{T}}(k))$. The eigendecomposition of $\mathbf{R}_{\mathbf{x}}$ is given by

$$\mathbf{R}_{\mathbf{x}} = \mathbf{U}\Lambda\mathbf{U}^{\mathrm{T}}. \tag{7}$$

The whitening transformation is expressed as

$$\mathbf{z}(k) = \mathbf{Q}\mathbf{x}(k), \tag{8}$$

where $\mathbf{Q} = \Lambda^{-1/2}\mathbf{U}^{\mathrm{T}}$. One can easily verify that $\mathbf{R}_{\mathbf{z}} = E(\mathbf{z}(k)\mathbf{z}^{\mathrm{T}}(k))$ is the identity matrix under this transformation. After the whitening transformation we have

$$\mathbf{z}(k) = \mathbf{Q}\mathbf{x}(k) = \mathbf{Q}\mathbf{A}\mathbf{s}(k) = \mathbf{B}\mathbf{s}(k), \tag{9}$$

where $\mathbf{B}$ is an orthogonal matrix, as verified by the following relation:

$$E\{\mathbf{z}(k)\mathbf{z}^{\mathrm{T}}(k)\} = \mathbf{B}E\{\mathbf{s}(k)\mathbf{s}^{\mathrm{T}}(k)\}\mathbf{B}^{\mathrm{T}} = \mathbf{B}\mathbf{B}^{\mathrm{T}} = \mathbf{I}. \tag{10}$$

We have therefore reduced the problem of finding an arbitrary full-rank matrix $\mathbf{A}$ to the simpler problem of finding an orthogonal matrix $\mathbf{B}$, which then gives

$$\hat{\mathbf{s}}(k) = \mathbf{B}^{\mathrm{T}}\mathbf{z}(k) = \mathbf{B}^{\mathrm{T}}\mathbf{Q}\mathbf{x}(k). \tag{11}$$

From Eqs. (6) and (11), the relation between $\mathbf{W}$ and $\mathbf{B}$ can be expressed as

$$\mathbf{W} = \mathbf{B}^{\mathrm{T}}\mathbf{Q}. \tag{12}$$

To calculate $\mathbf{B}$, it is initialized and then updated so that the projection, $\hat{\mathbf{s}}(k) = \mathbf{B}^{\mathrm{T}}\mathbf{z}(k)$, has to maximize non-Gaussianity. Hyvärinen (1999a) suggested a fast and robust fixed-point algorithm for ICA that entails maximizing the negentropy under the constraint of$\|\mathbf{b}_i\| = 1$, where $\mathbf{b}_i$ is the ith column of $\mathbf{B}$. A detailed description of the ICA algorithm based on maximizing the non-Gaussianity to calculate $\mathbf{B}$ can be found in the literature, Ref. [23]. After finding $\mathbf{B}$, the demixing matrix $\mathbf{W}$ can be obtained from Eq. (12).

The performance and interpretation of ICA monitoring depends on the correct choice of the ordering and dimension of the ICA model. The selection of a few key ICs has at least two advantages: robust performance and reduction of analysis complexity. One approach to choosing the dominant components is to separate the selection process into two steps:

Step 1. List and order all the ICs in the appropriate order.
Step 2. Select the first few ICs in the list as the dominant ones.

Unlike PCA, there is no standard criterion for ordering of ICs, which complicates the ordering procedure. A number of methods for ordering ICs have been suggested. In the present study, we used the simple approach of sorting the rows of the demixing matrix, **W**, on the basis of their Euclidean norms (L_2), where the L_2 norm of row $\mathbf{w}_i$ of **W** is:

$$\arg\ \underset{i}{\text{Max}}\|\mathbf{w}_i\|_2, \tag{13}$$

i.e., the ICs are sorted using an L_2 norm in order to show only those ICs that cause dominant changes in the process.

Once the ICs have been ordered, it is necessary to select the optimal number of ICs to be used for monitoring. This step is crucial because selecting too many ICs will magnify the noise and too small ICs will not be insufficient to catch the dominant characteristics of process, leading to poor monitoring performance. The data dimension can be reduced by selecting the first few rows of the ordered **W** based upon the assumption that the rows with the largest Euclidean norm have the greatest effect on the variation of **S**. This approach is based on the idea that the dominant variation in a process can be monitored by considering the cumulative sums of only the first few dominant ICs. We used a graphical technique to determine the number of ICs similar to the SCREE test of PCA [19,28].

3.2. Multiway independent component analysis (MICA)

In order to obtain better on-line batch monitoring performance, we developed an on-line MICA batch monitoring method that used another unfolding method and independent component analysis [19,20]. Similar to MPCA, the key idea is to exploit the ability of MICA to extract features from batch data by projecting the data onto a low-dimensional space. Following is the basic description of the MICA method (for detail, see the appendix). First, the normal batch data $\underline{X}(I(\text{batch}) \times J(\text{variable}) \times K(\text{time}))$ is unfolded to a matrix $(I \times JK)$ as in Nomikos and MacGregor's approach. Then mean centering and scaling is done to remove the mean batch trajectory and to attenuate the nonlinear dynamics. After eliminating the batch trajectory, the unfolded matrix $(I \times JK)$ is rearranged into a matrix with dimension $(IK \times J)$ as in the approach of Wold et al. [22]. Fig. 2 shows this new unfolding method. Subsequently, ICA is used to extract the underlying factors from this multivariate statistical data matrix $(IK \times J)$, where $\mathbf{X}_{\text{normal}}(J \times IK)$, **W** as well as $\mathbf{S}_{\text{normal}}$ are obtained from the FastICA algorithm ($\mathbf{S}_{\text{normal}} = \mathbf{W}\mathbf{X}_{\text{normal}}$). The matrices **B, Q,** and **A** are also obtained by whitening and the FastICA algorithm. The selected m rows of **W** constitute a reduced matrix $\mathbf{W}_{\text{d}}$ (deterministic part of **W**), and the remainder rows of **W** constitute a reduced matrix $\mathbf{W}_{\text{e}}$ (excluded part of **W**). We can construct matrix $\mathbf{B}_{\text{d}}$ and $\mathbf{B}_{\text{e}}$ by selecting the columns from **B** whose index corresponds to the indices of the selected rows of **W**. Most of the information of the process variables which capture linear and dynamic features of the underlying correlation structure in the data is contained in the total score matrix ($\text{I}_{\text{ICA}}(IK \times a)$ of the MICA model in Fig. 2. Based on the MICA model, new on-line data of a batch is projected into and compared with the normal operating model in real-time. Then, new independent matrices, $\mathbf{S}_{\text{newd}}$ and $\mathbf{S}_{\text{newe}}$ can be obtained if new data, **X**, is projected onto $\mathbf{W}_{\text{d}}$ and $\mathbf{W}_{\text{e}}$, respectively.

This method gives two merits for on-line batch monitoring. The future missing values do not have to be estimated and the batch length of each batch does not need to be aligned with other batches. Furthermore, process faults will be detected more easily than in Wold's method since the major nonlinear dynamics are eliminated by the batch trajectory elimination. Here, the dimensions of the loading vectors of the MICA model are small, the non-linear and dynamic features remain in the projected data in MICA, that is, the ICA source signals, whereas the loading matrices of MacGregor's approach are much larger because the loading matrices include all linear and dynamic process characteristics.

The implementations of the monitoring statistics of MICA are similar to those of the monitoring statistics of MPCA. In MICA, three types of statistics are calculated from the process model in normal operation: the D-statistic (I^2) for the systematic part of the process variation, a second I^2 metrics (I_e^2) based on excluded ICs and the Q-statistic for the residual part of the process variation [19]. The I^2 statistic for sample k is the sum of the squared independent scores and is defined as follows:

$$I^2(k) = \mathbf{s}(k)^{\text{T}}\mathbf{s}(k), \tag{14}$$

where $\mathbf{s}(k)$ is the kth column vector of **S**. Also, we can calculate the I^2 metric of the excluded independent components, that is, the I_{e}^2 metric. The I_{e}^2 statistic can be defined as follows:

$$I_{\text{e}}^2(k) = \mathbf{s}_{\text{e}}(k)^{\text{T}}\mathbf{s}_{\text{e}}(k), \tag{15}$$

where $\mathbf{s}_{\text{e}}(k)$ is the kth column vector of $\mathbf{S}_{\text{e}}$. Monitoring the non-systematic part of the measurements provides an additional fault detection tool, which can detect special events entering the system. The I_{e}^2 statistic has the further advantage that it can compensate for the error that results when an incorrect number of ICs is selected for the dominant part. The use of I^2 and I_{e}^2 statistics allows the entire space spanned by the original variables to be monitored through a new basis.

The SPE statistic for the nonsystematic part of the common cause variation of new data can be visualized in a chart with confidence limits. The SPE statistic at

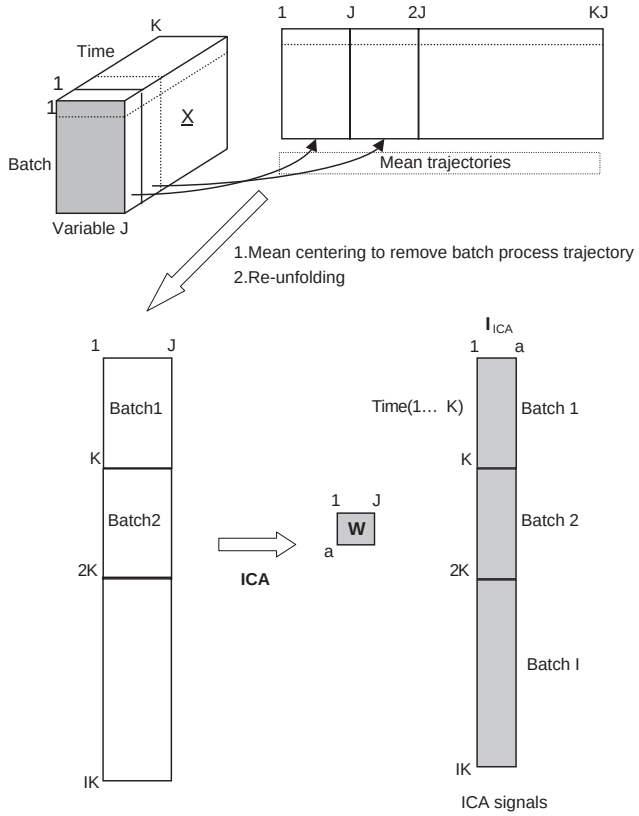

Fig. 2. MICA monitoring method that combines a new unfolding three-way batch data and a feature extraction of ICA.

sample k is defined as follows:

$$\mathrm{SPE}(k) = \sum_{j=1}^{d} (x_j(k) - \hat{x}_j(k))^2, \tag{16}$$

where SPE(k) is defined as the sum of the squares of $\mathbf{e}(k)$ [the columns of $\mathbf{E}$ in Eq. (7)], d is the number of variables of data matrix $\mathbf{X}$, $x_j(k)$ is the entry in the jth row and kth column of $\mathbf{X}$ and $\hat{x}_j(k)$ is the predicted value of the MICA model which is the entry in the jth row and kth column of $\hat{\mathbf{X}}$. $\hat{\mathbf{X}}$ can be calculated as follows:

$$\hat{\mathbf{X}} = \mathbf{Q}^{-1}\mathbf{B}_{\mathrm{d}}\mathbf{S}_{\mathrm{d}} = \mathbf{Q}^{-1}\mathbf{B}_{\mathrm{d}}\mathbf{W}_{\mathrm{d}}\mathbf{X}. \tag{17}$$

The SPE statistic is a measure of lack of fit with the constructed MICA model. Thus the residuals account for any variability which is not described sufficiently in the database of normal batches. A new test batch with a high SPE is not 'modeled' by the model and was not represented in the normal batches. The appendix describes the detailed on-line batch MICA monitoring method (Fig. 2).

4. Materials and methods

The data used in this research were collected from a pilot-scale SBR system shown in Fig. 3. A fill-and-draw SBR with a 80-l working volume is operated in a 6 h cycle mode and each cycle consists of fill/anaerobic(1 h), aerobic(2 h 30 min), anoxic (1 h), re-aerobic(30 min) and settling/draw(1 h) phases. The hydraulic retention time (HRT) and the solid retention time (SRT) are maintained at 12 h and 10 days, respectively. Loading amounts of chemical oxygen demand (COD) as synthetic municipal-like sewage, NH_4^+-N, PO_4^{3-} per cycle in standard conditions are 440, 60 and 95 mg/l, respectively.

The control of the duration/sequence of phases and on/off status of peristaltic pumps, mixer and air supply are automatically achieved by a Labview data acquisition and control (DAC) system. The DAC system consists of computer, analog/digital interface cards, sensors, transmitters and solid state relays (SSR). Electrodes for pH, oxidation–reduction potential, dissolved oxygen (DO), temperature, weight and conductivity in Table 1 are installed and connected to the individual sensors. The status of the SBR reactor is

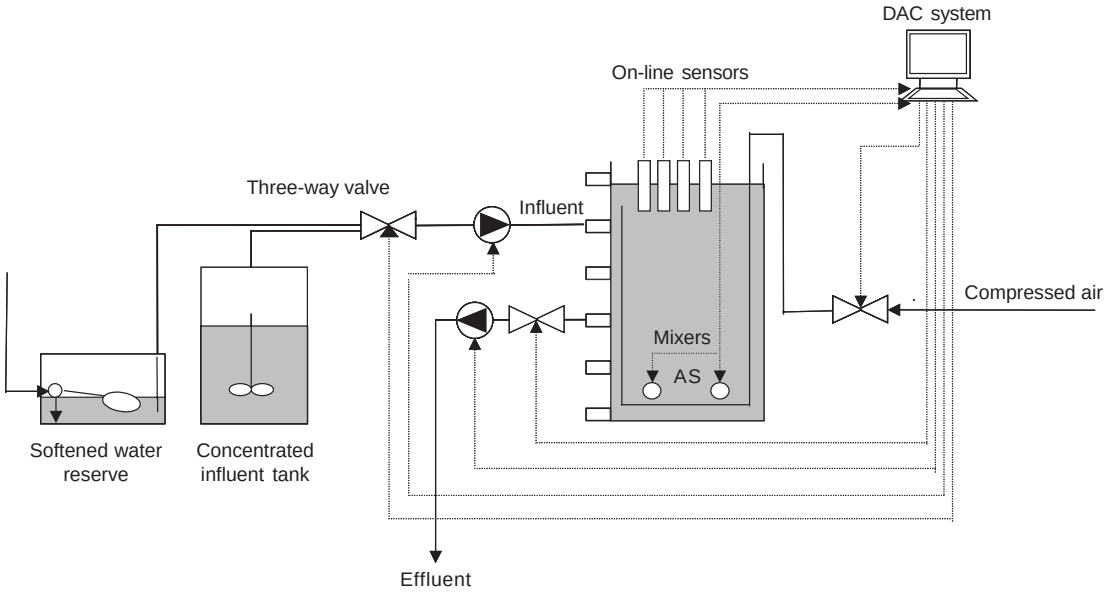

Fig. 3. Schematic diagram of bench-scale sequencing batch reactor.

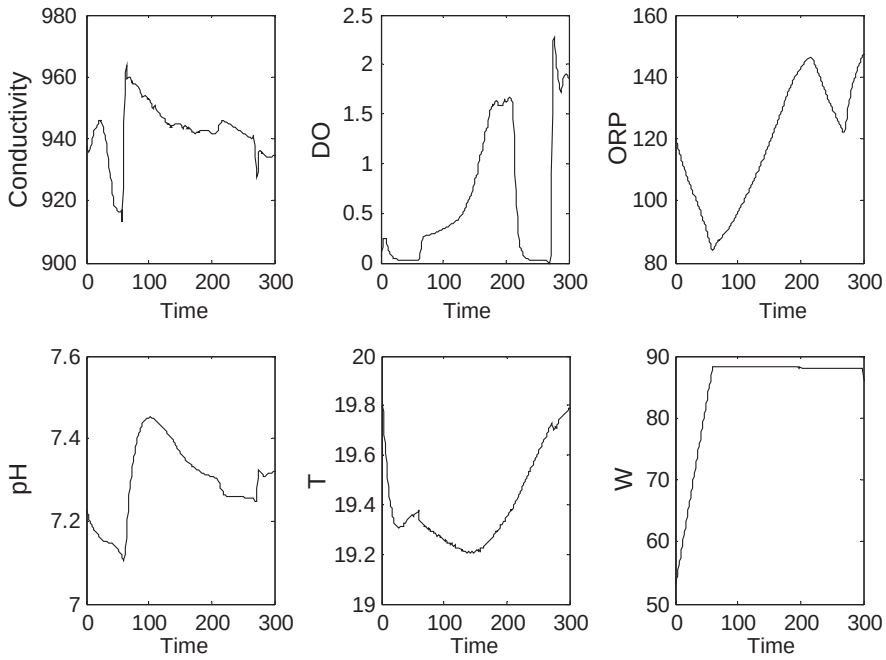

Fig. 4. Typical batch trajectory profiles of a SBR.

displayed on the computer and the sensor signals are stored. A set of on-line measurements is obtained every 1 min (360 times points per cycle). These measurements of SBR reactor were stored for 70 days (280 cycles), which constructed a database of historical information [3]. Only the first 300 sampling time instants were used to develop the model during normal operating condition (NOC), since biological reactions in the settling and drawing phases (corresponding to those of the last 60 time instants) were assumed as negligible. Moreover, the sensor signals were unreliable due to the absence of mixing.

5. Result and discussion

5.1. MPCA analysis of historical SBR data set

Fig. 5 shows the Hotelling's T^2 and SPE charts of all 280 batches using the MPCA method with the six original variables. The MPCA model for on-line monitoring was developed from the historical data set of the selected 144 batches to create a rather broad scope of normal batches, where six abnormal batches (batch number: 61, 69, 85, 86, 99 and 100) were excluded for the NOC model. Four principal components were retained by the cross-validation method, which explained approximately 81% of the total variability in Table 2. The test data set that consisted of the remaining 130 batches were projected onto the reduced MPCA model space. The T^2 chart of Fig. 5 rarely exceeds its limit, whereas the SPE chart is far above the 99% limit from batch 190 on. It is well known that changes in the relationships between variables, such as sensor faults, tend to be detected on the SPE chart, while changes in operating conditions, for example a grade change and an evolution of new operating condition, are typically identified on the T^2 chart. However, the MPCA model may not be valid because the NOC model is not representative of the SBR process because it does not

Table 1
Real-time measured variables of a SBR

No.	Variables
1	Conductivity (mS)
2	Dissolved oxygen concentration (mg/l)
3	Oxidation reduction potential (mV)
4	pH
5	Temperature (°C)
6	Weight (g)

Table 2
Percent variance captured by MPCA model

	MPCA model	
PC number	% Variance of this PC	% Variance captured total
1	31.3	31.3
2	23.2	54.5
3	15.18	69.68
4	11.39	81.07

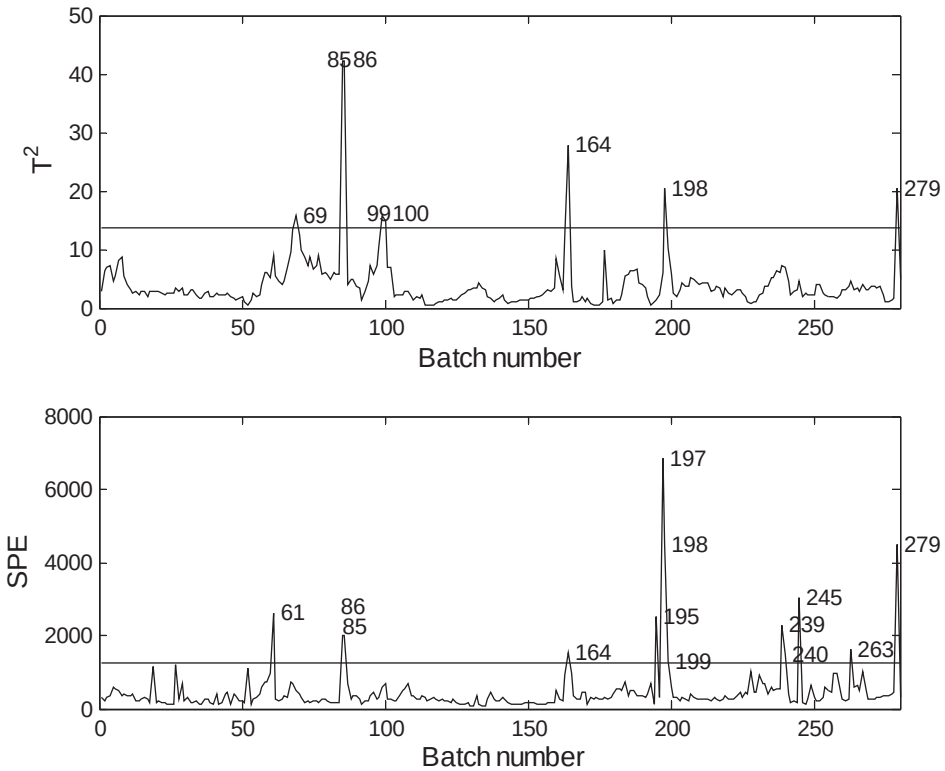

Fig. 5. T^2 and SPE plots of all 280 batches using the MPCA method with the original variables. The dotted lines correspond to 99% confidence limit.

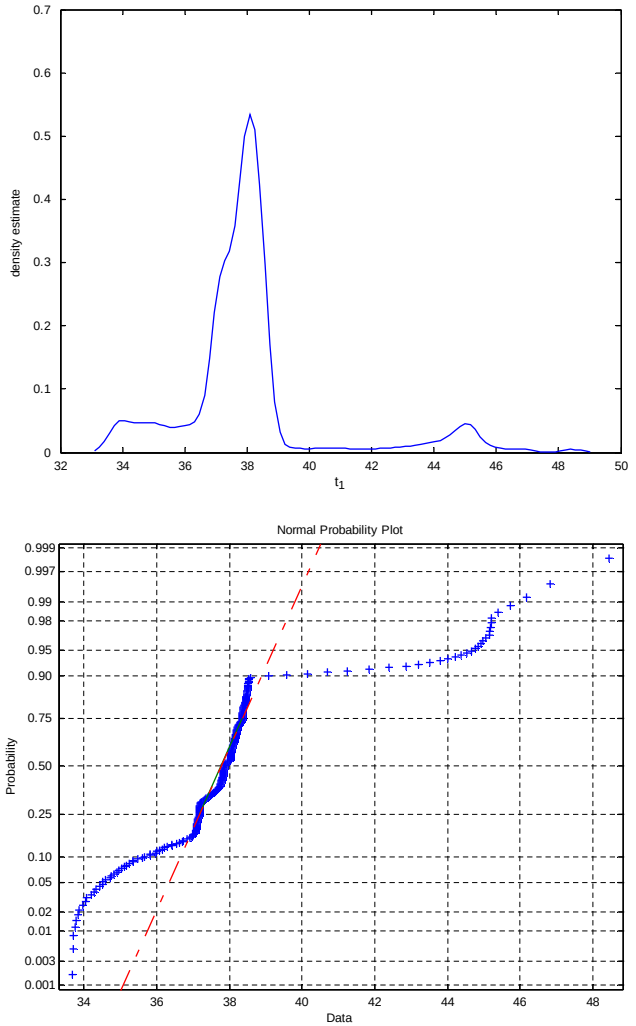

Fig. 6. Non-Gaussian distribution of the first score (t_1) obtained from MPCA (a) density estimate (b) normality check.

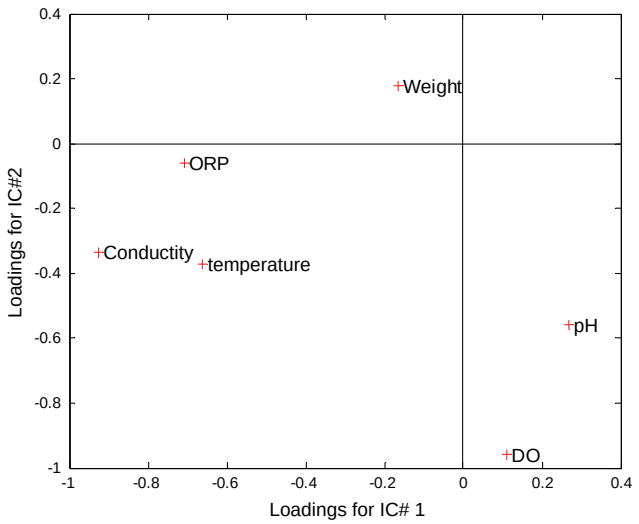

Fig. 7. Loading plot of the MICA method: IC_1 vs. IC_2

follow the Gaussian distribution due to the time-varying characteristics of SBR process.

Fig. 6 shows that the density estimates of the first score (t_1) in MPCA does not follow the Gaussian distribution but the '*supergaussian distribution*' in which random variables take relatively more often values that are very close zero or very large. Thus, the T^2 and SPE charts of MPCA that are based on the assumption that the data are Gaussian distributed may cause a false result when used for monitoring. Note that the T^2 and SPE statistics do not depend on a certain distribution, only their confidence limits. Because non-Gaussian data may inflate the variance, it tends to reduce the T^2 statistics. Typically, this increases the false alarm rate of

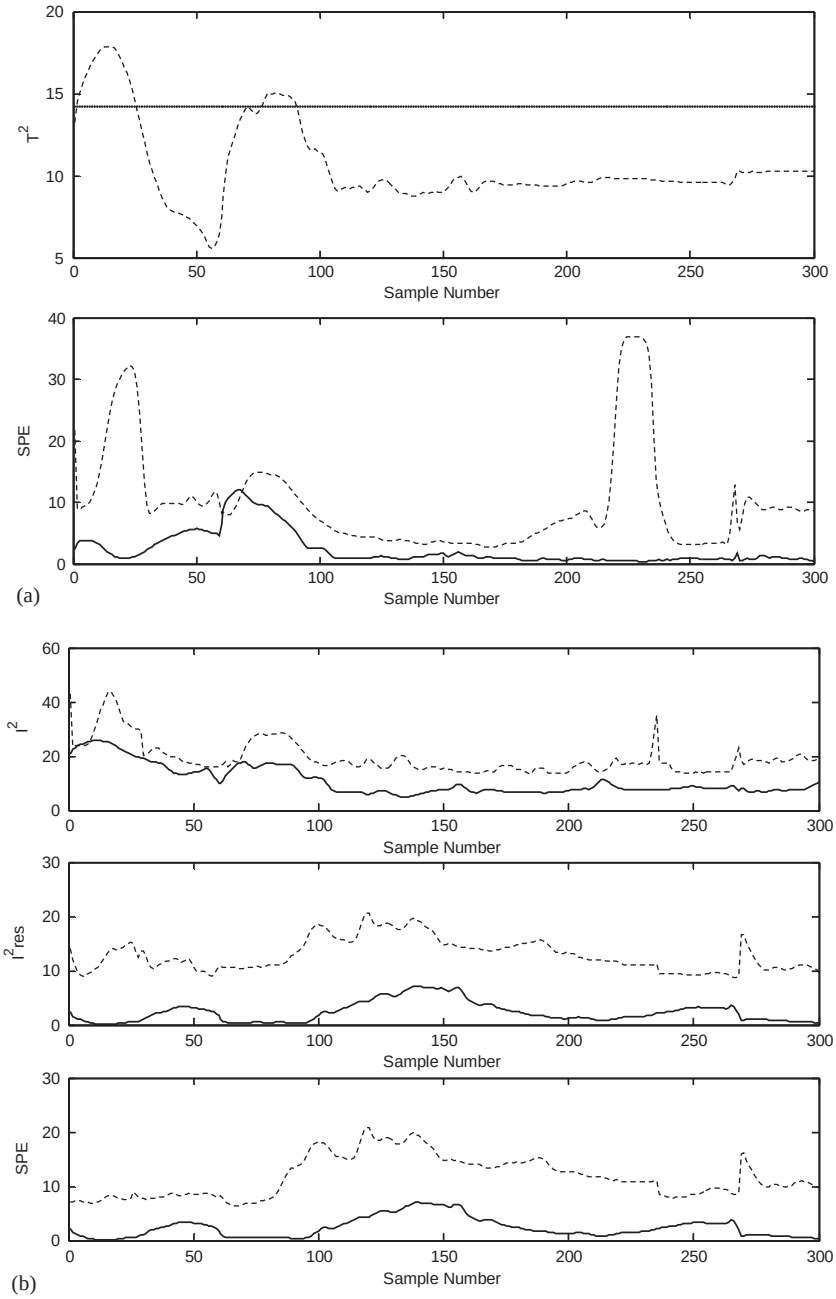

Fig. 8. On-line monitoring charts for *normal* batch 161: (a) T^2 and SPE charts of MPCA with 99% control limits (dashed), (b) I^2, I_e^2 and SPE charts of MICA with 99% control limits (dashed).

the MPCA which a normal batch might be judged as a non-conforming one. Obviously, this deteriorates the reliability of the multivariate monitoring system and makes it subject to unfavorable criticism. On-line monitoring on multivariate methods is often an issue of minimizing the number of false alarms while true deviations are retained and detected. Robust limits can be determined empirically using kernel density estimation as used in this paper [29]. Moreover, if the batch length of a new batch is different from the length of old batches, the on-line monitoring method based on MPCA cannot be applied. Actually, many real-world data sets have a super-Gaussian distribution in which the probability density of the data is peaked in the middle and has heavy tails (large values far from zero), when compared to a Gaussian density with the same variance. This observation is the motivation of the ICA model. ICA is sensitive to modes whose influences on the measured variables follow a super-Gaussian distribution with large tails and a pronounced peak in the middle.

5.2. *On-line monitoring and fault diagnosis using MPCA and MICA*

MPCA and MICA models are used to monitor the SBR process with a historical data set. Four principal components were selected for the MPCA model while four independent components were chosen for the MICA model. To estimate the future values in $\mathbf{X}_{new}$, we used the estimation method 2, which fills in all future measurements with the current deviation from the average batch. Then the MPCA and MICA models are tested against a new batch using a 99% control limit. A new batch of SBR are monitored for every time point k with the monitoring charts based on the MPCA and MICA models.

Fig. 7 represents the loading plot of the MICA method to see how the variables are interrelated. It is important to point out that Fig. 7 only partly represents the interrelation between the variables since the interrelation depicted in Fig. 7 is only representing 2 out of 4 dimensions. Two process variables (ORP, temperature) give the same direction and are located in a similar position in the reduced MICA model space, where they show similar dynamic behavior within a batch as illustrated in Fig. 4. The weight variable does not correlate with the other variables since the weight only increases in the filling phase and remains constant irrespective of the operation status. Similar to the MPCA method, the biological interpretation of MICA is meaningful to the multivariate analysis of batch processes in case of non-Gaussian distributions.

Fig. 8 shows the on-line monitoring results of the T^2 and SPE charts of MPCA and the I^2, I_e^2 and SPE charts of MICA with 99% confidence limits calculated by the kernel density estimation method for the *normal* batch 161. The MICA result shows that the I^2, I_e^2 and SPE statistics for this batch are within the control limits for the whole duration of the batch run. Therefore, this batch in MICA is assigned as being "in control" or "normal". But the T^2 and SPE charts of MPCA exceed the upper control limits two times, in the beginning and around the 60th sampling time. It is due to the inexact filling in the batch start period and due to the non-Gaussian distributed data during the phase change (from anaerobic to aerobic). On the other hand, the SPE

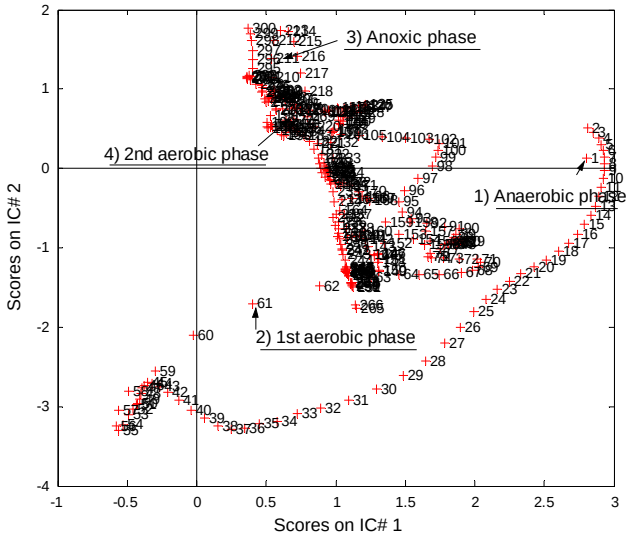

Fig. 9. Score plot of the MICA method for a normal SBR operation (batch 161) in IC_1–IC_2 plane: It represents time profile of a normal operating batch with the MICA model.

chart of MPCA moves up and down four times from the beginning of a batch to the end time of SBR process since the operating conditions of SBR process have a unique cyclic batch operation (anaerobic, first aerobic, anoxic and second aerobic phases). The I^2 chart of MICA shows similar trend to the SPE chart of MPCA. It illustrates that the selected independent components in ICA can exactly extract the dynamic characteristics of

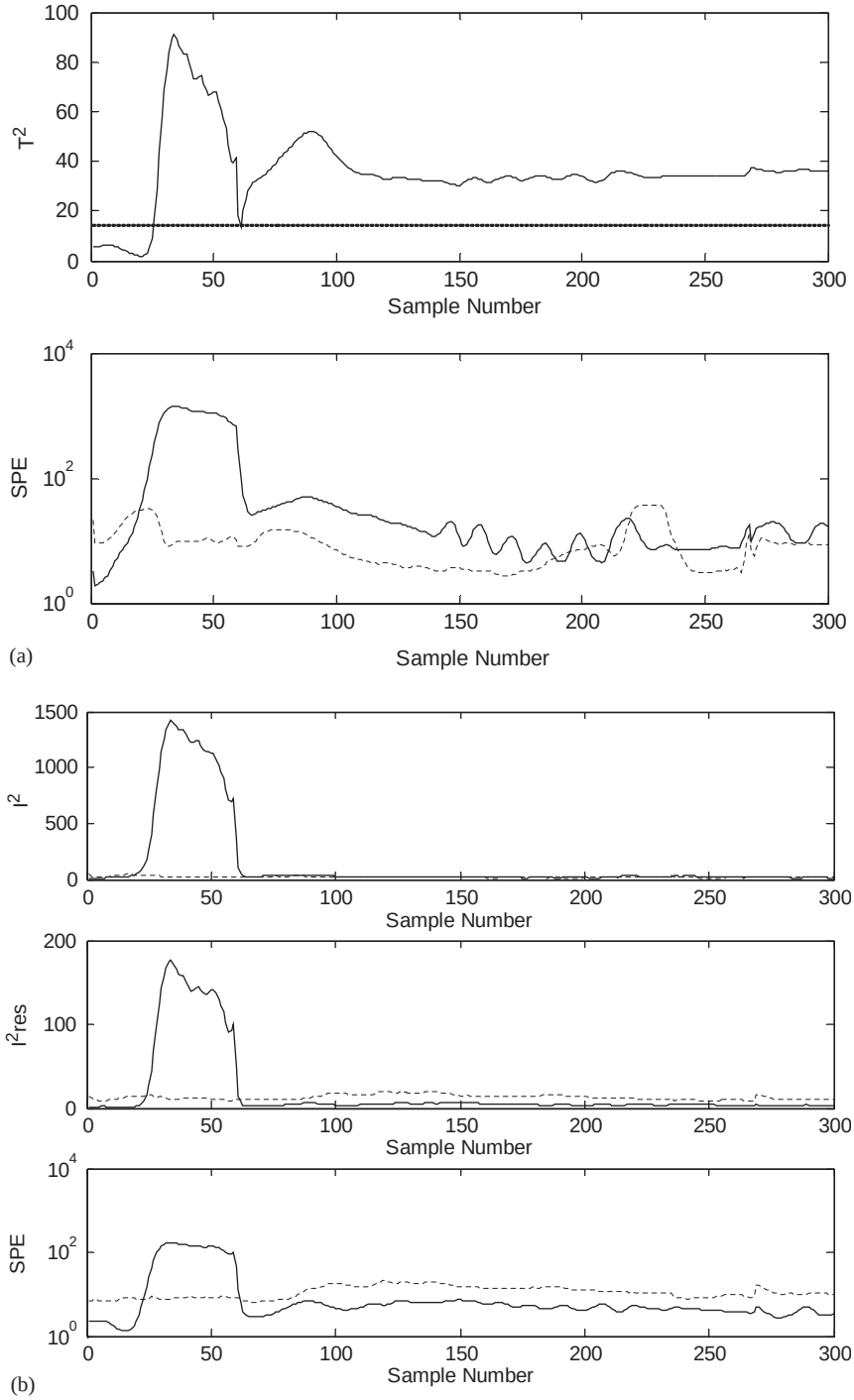

Fig. 10. On-line monitoring charts of MPCA for *abnormal* batch number 245: (a) T^2 and SPE charts of MPCA with 99% control limits (dashed), (b) I^2, I_e^2 and SPE charts of MICA with 99% control limits (dashed).

the SBR operation, i.e. the extracted dynamic characteristics of the SBR operation move from the SPE chart of MPCA to the I^2 chart of MICA. The control limits of the I^2 chart also result in wide confidence intervals in the beginning of the batch and narrow confidence intervals at the end of batch. The initial conditions of startup in SBR have different values for each batch. These cause some variations in the process variables at the start of the batch. Then the SBR is controlled using a set point trajectory until the end of the batch. Therefore, variations are large in the start stage of batches, whereas variations in the late stage of batches are low. For this reason, the *SPE* control limits of the MPCA and MICA models have wide confidence intervals at the beginning of a batch and narrow confidence intervals at the end of a batch. It shows that the statistics of the MICA model represent the biological phenomena and their relationships, which occur during the batch. Moreover, contrary to the MPCA model, the *D*-statistics of the I^2 and I_e^2 charts have control limits at each sampling time. These characteristics which consider the confidence limits at every time of each batch increase the on-line monitoring performance of the MICA method.

Fig. 9 gives the time evolution of a *normal* SBR operation: batch 161, where the phase trajectory of SBR operation is given by the four phase names. The anaerobic phase ($t = 0 - 60$ min) starts from the right middle side of the ICA plane, evolves through the lower side of IC_2 and ends in the middle of the ICA plane. The first aerobic phase ($t = 61 - 210$ min) starts from the middle of the ICA plane and evolves across the first independent component axis (IC_1). The anoxic phase ($t = 210 - 270$ min) starts in the first quarter of the ICA plane and evolves across the first independent component axis (IC_1). And the second aerobic phase ($t = 271 - 300$ min) starts in first quarter plane of the ICA plane and evolves within the first quarter ICA plane. As previously mentioned, with the used unfolding method, it is possible to monitor the progression of the batch operation in a reduced ICA plane, where statistical control limits allow to identify anomalous process behaviors and their time intervals and possible causes.

Fig. 10 represents the on-line monitoring results with T^2 and SPE charts of the MPCA model and the I^2, I_e^2 and SPE charts of the MICA model with 99% confidence limits calculated by the kernel density estimation method for an *abnormal* batch 245. The DO concentration in the batch 245 in Fig. 13 increased too early in the anaerobic phase because the air bubble was beneath the DO sensor and returned to the normal concentration during the aerobic phase because the aeration got rid of the air bubble. Both the MPCA and MICA methods show similar detection times in this batch. However, the monitoring result of MPCA calls

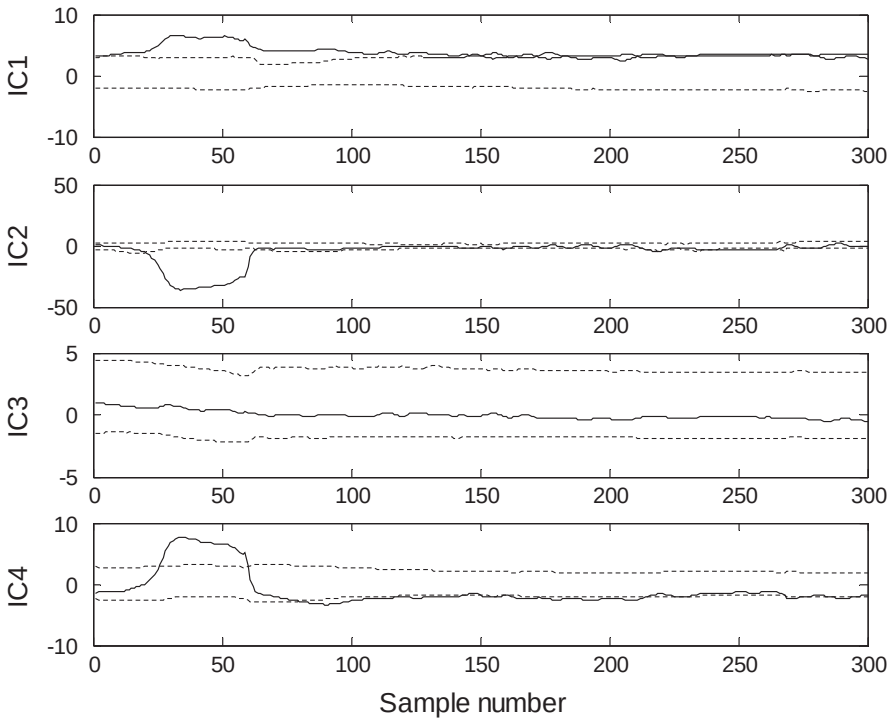

Fig. 11. Monitoring charts of individual ICs for *abnormal* batch number 245: IC_1, IC_2, IC_3 and IC_4 charts with 99% control limits.

that the fault continues until the end of the batch. That is, because the on-line monitoring method of MPCA needs to predict the future observations in order to fulfill the incomplete data sets, anticipating the future observation might cause this lasting false fault detection. However, the predicted value should consider the dynamic relationship, otherwise, it may distort the data information. On the other side, Fig. 10(b) shows that the I^2 chart of MICA detects a significant deviation from the batch start time. Also both the I_e^2 and SPE charts of MICA can detect this fault during the anaerobic phase and return within the control limits after the aerobic phase. In most industrial productions where batch processes are used, the occurrence of a fault means that the batch is immediately rejected (e.g. in the pharmaceutical and food industry). However, this is not the case in wastewater treatment since there is no (or little) control of the influent flow and poorly treated water is better than non-treated water. Thus, when a fault is detected, the batch run will carry on and operators will

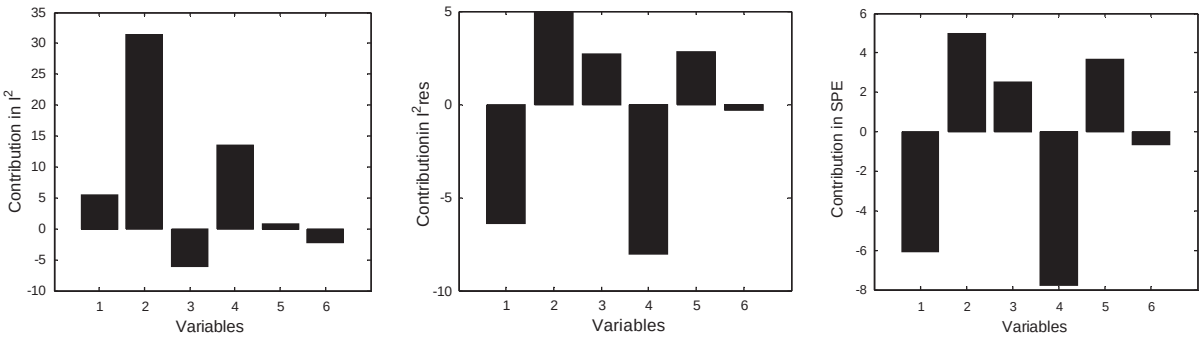

Fig. 12. Contribution plots of MICA for *abnormal* batch number 245 at sample time 45: I^2, I_e^2 and SPE statistics.

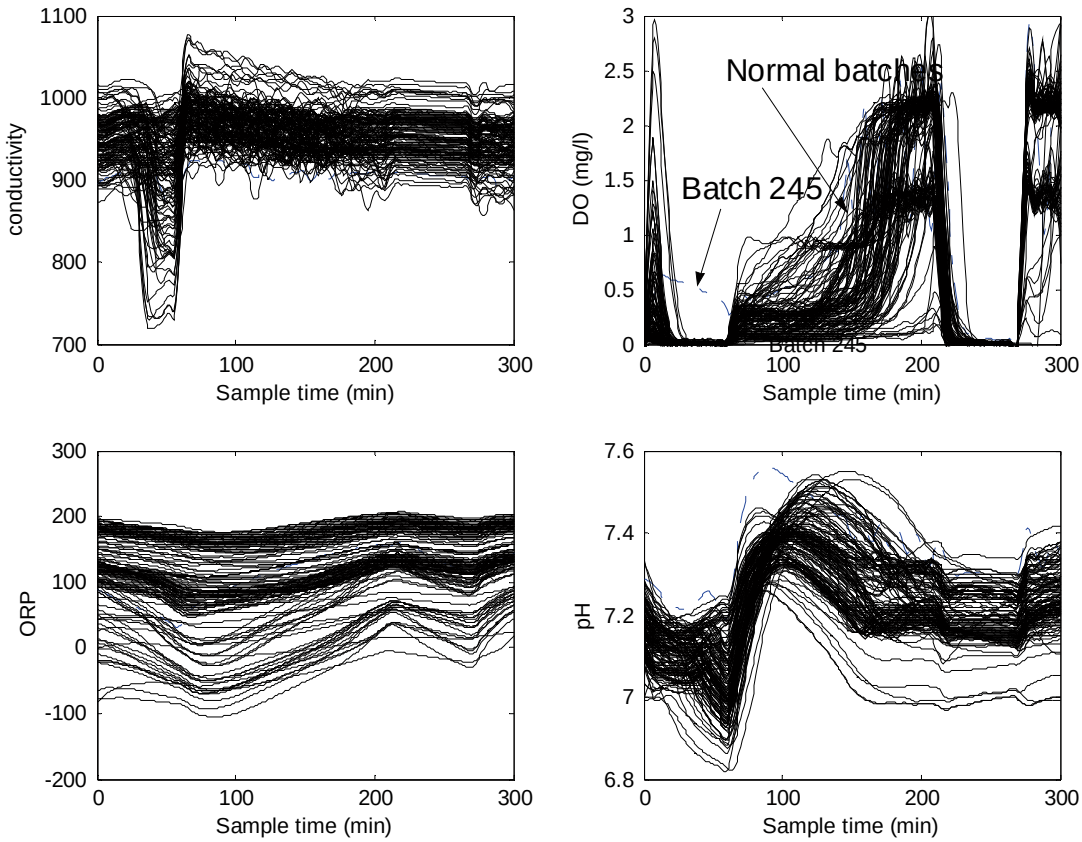

Fig. 13. The univariate plots of conductivity, DO, ORP and pH for normal batches and batch 245.

use the information on the fault to correct the following batch.

Fig. 11 shows the individual independent component in the abnormal batch 245 to get a better understanding of the batch operation. The low and high control limits were calculated using the kernel density estimation method with a 99% confidence limit. If a fault was detected, the individual plot of ICs can be checked to get a better understanding of fault sources. It is notable to see that the fault is first detected in the first independent component (IC_1). From this fact, it is possible to recognize the independent component in the individual IC plots corresponding to a particular kind of faults and to build a knowledge-based expert system for fault diagnosis.

Once a fault or special event has been detected, it is important to diagnose the event to find an assignable cause. For this, contribution of each measurement variable to the deviations observed in the monitoring metric can be displayed. These contribution or diagnostic charts can be immediately displayed on-line by the operator as soon as the special event is detected. Although they may not provide an unequivocal diagnosis, they at least will clearly show the group of variables that are primarily responsible for the detected deviations. In Fig. 12, contribution plots for the I^2, I_e^2, and SPE charts are displayed. From the contribution plot for the I_e^2 and SPE charts at sample 45, we can conclude variable 1 (conductivity), 4 (pH) as well as variable 2 (DO) are primarily contributing to the I^2, I_e^2 and SPE statistics. Fig. 13 shows the univariate plots of conductivity, DO, ORP and pH for normal batches and batch 245. The DO concentration in the batch 245 increased too early in the anaerobic phase because the air bubble was beneath the DO sensor.

5.3. On-line monitoring using multiple MICA sub-models

Although the MICA model uses another unfolding method compared with MPCA, the monitoring results according to time are not distorted since the time correlation of the variables is attenuated by the mean trajectory removal of variables at each time. If the time correlation of variable is very strong, it may be

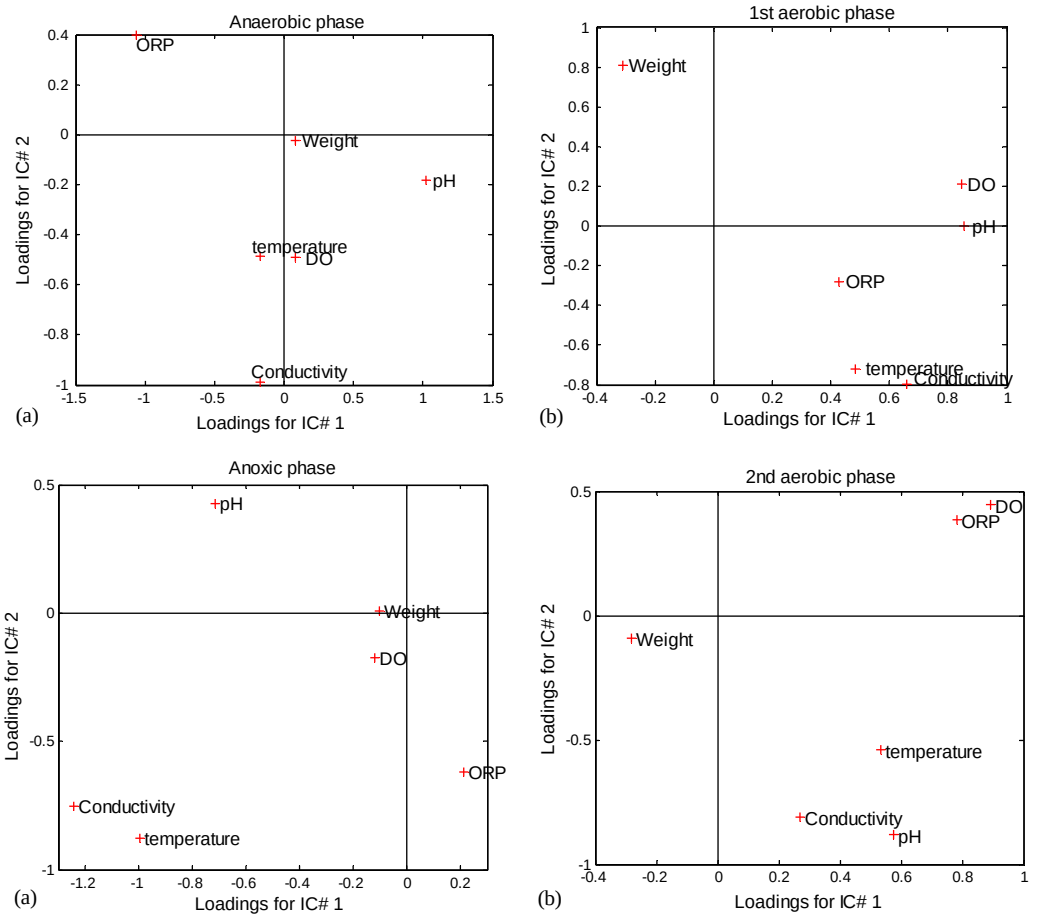

Fig. 14. Loading plot of the MICA method using sub-models: (a) anaerobic, (b) first aerobic, (c) anoxic and (d) second aerobic.

appropriate to use separate models for each batch phase [6]. This means that the data distribution can change for each phase during the batch operation. This multi-phase monitoring method can give us a faster detection and easier fault isolation. Because the SBR consists of several phases in each cycle, there are different statistical properties for the different phases. Statistics between variables that are valid at the start of a batch may not hold towards the end of the batch. These characteristics can be solved by constructing multiple sub-models for multiphase. Figs. 14 and 15 show the loading plots and on-line monitoring results of MICA using four sub-models for the abnormal batch 245. Because SBR is composed of several phase operation which is more focused on the local behavior of the batch process, the multiple sub-model approach could be appropriate for the SBR process. The difference in the statistical distribution structure in each phase can be found in the loading plot in Fig. 14. It provides information about the detail change of statistical relationships within each phase. As shown in Fig. 15, on-line results of MICA with the four sub-models show a more rapid detection capability and allow for easier interpretation of SBR operation. It is able to localize the cause of faults or disturbances and gives a much clearer indication of the process disturbances or faults.

In summary, the capability difference between the MPCA and MICA methods mainly originates from the extracted feature components. Both methods find hidden information from the multidimensional data set. While PCA looks for Gaussian components, ICA searches for non-Gaussian components. If a data set contains any non-Gaussian component, ICA can show better feature extraction performance than PCA. Therefore, ICA may improve the monitoring performance by extracting the key hidden variables that influence the process.

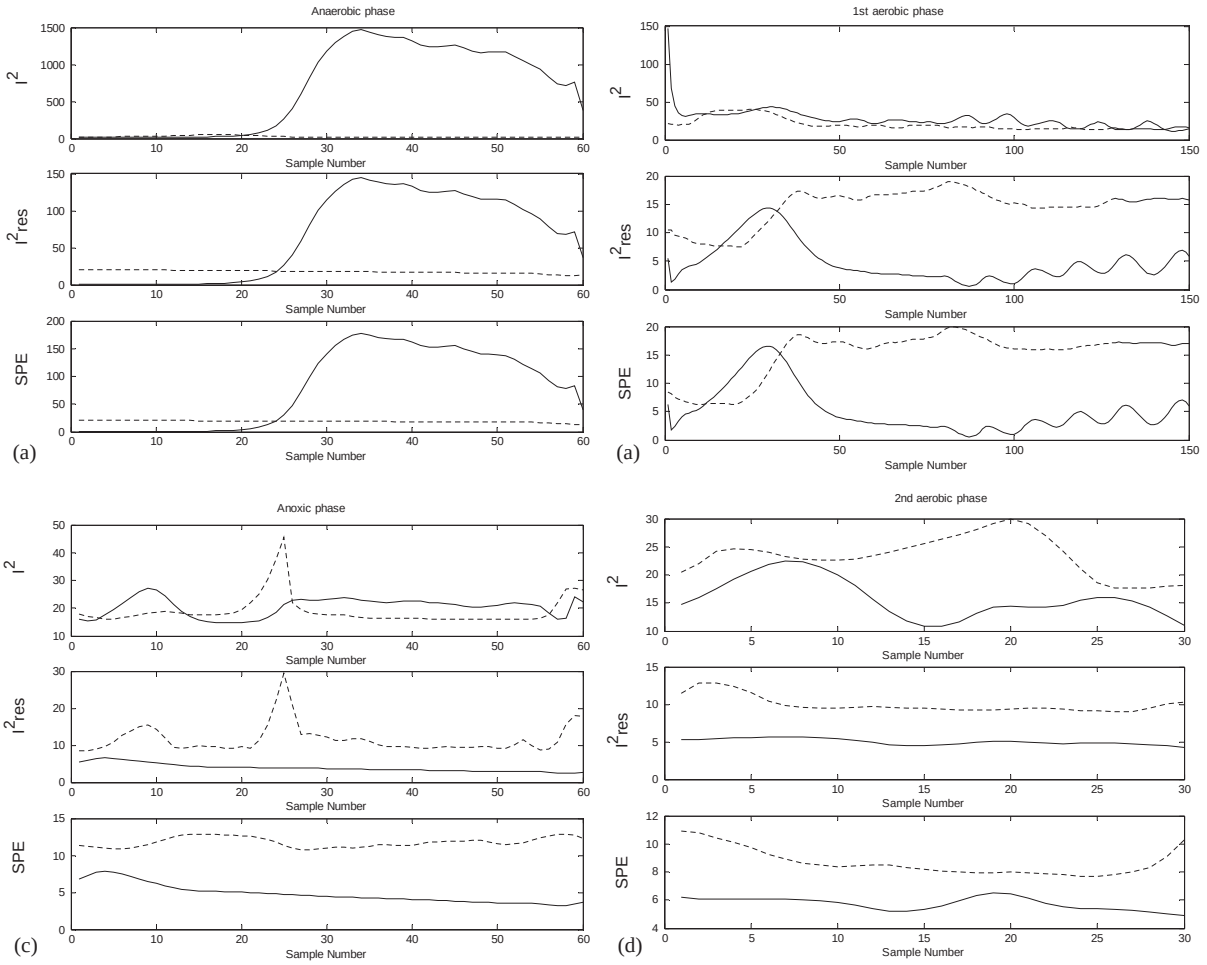

Fig. 15. On-line monitoring charts of MICA using sub-models for *abnormal* batch number 245: I^2, I_e^2 and SPE charts with 99% control limits.

6. Conclusions

The SBR poses an interesting challenge for process monitoring of systems characterized by nonstationary, batchwise, multiscale, and non-Gaussian characteristics. An application for monitoring the progress on SBR using the MICA method has been presented. The MICA method allows to monitor the time progression of the different batches in a reduced plane where statistical control limits allow to identify anomalous process behaviours and their time intervals and possible causes. Since ICA is not requiring that the latent variables be normally distributed, MICA can extract more important underlying independent factors from correlated data than MPCA. The application of the MICA monitoring method to a SBR process has demonstrated its efficiency and also showed better monitoring performance than an MPCA approach.

Acknowledgements

This work was financially supported by the Post-doctoral Fellowship Program of the Korea Science and Engineering Foundation (KOSEF) and a Visiting Post-doctoral Fellowship of the Fund for Scientific Research-Flanders (FWO).

Appendix A. On-line batch MICA monitoring

Following are the detailed procedure of the on-line MICA monitoring method [19,20].

A.1. Develop normal operating condition (NOC) model

1. Acquire normal operating data set during batch operation.
2. Unfold $\underline{\mathbf{X}}(I \times J \times K)$ to $\mathbf{X}(I \times JK)$.
3. The data $\mathbf{X}(I \times JK)$ are normalized using the mean and standard deviation of each variable at each time in the batch cycle over all batches.
4. Rearrange the scaled $\mathbf{X}(I \times JK)$ to $\mathbf{X}_{\text{normal}}(J \times IK)$.
5. Whitening procedure

$$\mathbf{Z}_{\text{normal}} = \mathbf{Q}\mathbf{X}_{\text{normal}}. \tag{A.1}$$

6. ICA procedure:

obtain $\mathbf{W}$, $\mathbf{B}$, and $\mathbf{S}_{\text{normal}}$ from $\mathbf{S}_{\text{normal}} = \mathbf{W}\mathbf{X}_{\text{normal}} = \mathbf{B}^{\text{T}}\mathbf{Z}_{\text{normal}}$.

7. Calculate the norm of the row vectors of $\mathbf{W}$ and separate $\mathbf{W}$ into the deterministic part and the excluded part based on the magnitude of norms. $\mathbf{B}$ and $\mathbf{S}_{\text{normal}}$ can be separated with the same criterion:

$$\mathbf{W} \rightarrow \mathbf{W}_{\text{d}}, \mathbf{W}_{\text{e}}, \tag{A.2}$$

$$\mathbf{B} \rightarrow \mathbf{B}_{\text{d}}, \mathbf{B}_{\text{e}}, \tag{A.3}$$

$$\mathbf{S}_{\text{normal}} \rightarrow \mathbf{S}_{\text{d}}, \mathbf{S}_{\text{e}}. \tag{A.4}$$

8. Calculate I^2, I_{e}^2, and SPE metrics:

$$I^2(n) = \mathbf{s}_{\text{d}}(n)^{\text{T}}\mathbf{s}_{\text{d}}(n), \tag{A.5}$$

$$I_{\text{e}}^2(n) = \mathbf{s}_{\text{e}}(n)^{\text{T}}\mathbf{s}_{\text{e}}(n), \tag{A.6}$$

$$\text{SPE}(n) = \sum_{j=1}^{d}(x_j(n) - \hat{x}_j(n))^2, \tag{A.7}$$

where n is a value from 1 to IK and $\hat{\mathbf{X}} = \mathbf{Q}^{-1}\mathbf{B}_{\text{d}}\mathbf{S}_{\text{d}} = \mathbf{Q}^{-1}\mathbf{B}_{\text{d}}\mathbf{W}_{\text{d}}\mathbf{X}_{\text{normal}}$.

9. Rearrange $I^2(1 \times IK)$, $I_{\text{e}}^2(1 \times IK)$ and $\text{SPE}(1 \times IK)$ to $I^2(I \times K)$, $I_{\text{e}}^2(I \times K)$ and $\text{SPE}(I \times K)$, respectively.
10. Obtain control limits of I^2, I_{e}^2 and SPE metrics at each time using kernel density estimation.
11. Obtain control limits of individual IC at each time using kernel density estimation in order to identify the cause of the faults.

A.2. On-line monitoring

1. For a new batch data until time $k, \mathbf{X}_{\text{new}}(k \times J)$, unfold it to $\mathbf{x}_{\text{new}}^{\text{T}}(1 \times Jk)$. Apply the same scaling used in modeling.
2. Scaled $\mathbf{x}_{\text{new}}^{\text{T}}(1 \times Jk)$ is rearranged into $\mathbf{X}_{\text{new}}(J \times k)$.
3. Calculate $\mathbf{s}_{\text{newd}}(k)$ and $\mathbf{s}_{\text{newe}}(k)$ from $\mathbf{s}_{\text{newd}}(k) = \mathbf{W}_{\text{d}}\mathbf{X}_{\text{new}}$, $\mathbf{s}_{\text{newe}}(k) = \mathbf{W}_{\text{e}}\mathbf{X}_{\text{new}}$.
4. Calculate $I_{\text{newd}}^2(k)$, $I_{\text{newe}}^2(k)$, and $\text{SPE}(k)$

$$I_{\text{newd}}^2(k) = \mathbf{s}_{\text{newd}}(k)^{\text{T}}\mathbf{s}_{\text{newd}}(k), \tag{A.8}$$

$$I_{\text{newe}}^2(k) = \mathbf{s}_{\text{newe}}(k)^{\text{T}}\mathbf{s}_{\text{newe}}(k), \tag{A.9}$$

$$\text{SPE}(k) = \sum_{j=1}^{d}(x_{\text{newj}}(k) - \hat{x}_{\text{newj}}(k))^2, \tag{A.10}$$

where $\hat{\mathbf{x}}_{\text{newj}}(k) = \mathbf{Q}^{-1}\mathbf{B}_{\text{d}}\mathbf{S}_{\text{newd}} = \mathbf{Q}^{-1}\mathbf{B}_{\text{d}}\mathbf{W}_{\text{d}}\mathbf{x}_{\text{new}}$.

A.3. Contribution plot

Once a fault is detected by the statistical monitoring method, the key approach to fault isolation using the MICA model is the use of contribution plots. The following three equations is to calculate the variable contribution for $I_{\text{newd}}^2(k)$, $I_{\text{newe}}^2(k)$ and $\text{SPE}(k)$:

1. Variable contribution for $I_{\text{newd}}^2(k)$

$$\mathbf{x}_{\text{cd}}(k) = \frac{\mathbf{Q}^{-1}\mathbf{B}_{\text{d}}\mathbf{s}_{\text{newd}}(k)}{\|\mathbf{Q}^{-1}\mathbf{B}_{\text{d}}\mathbf{s}_{\text{newd}}(k)\|}\|\mathbf{s}_{\text{newd}}(k)\|. \tag{A.11}$$

2. Variable contribution for $I^2_{newe}(k)$

$$\mathbf{x}_{ce}(k) = \frac{\mathbf{Q}^{-1}\mathbf{B}_e\mathbf{s}_{newe}(k)}{||\mathbf{Q}^{-1}\mathbf{B}_e\mathbf{s}_{newe}(k)||}||\mathbf{s}_{newe}(k)||. \quad \text{(A1.2)}$$

3. Variable contribution for SPE(k)

$$\mathbf{x}_{cspe}(k) = \mathbf{x}(k) - \hat{\mathbf{x}}(k). \quad \text{(A.13)}$$

References

[1] Mace M, Mata-Alvarez A. Utilization of SBR technology for wastewater treatment: an overview. I&EC 2002;41: 5539–53.

[2] Cohen A, Hegg D, Michele MD, Song Q, Kasabov N. An intelligent controller for automated operation of sequencing batch reactors. Water Sci Technol 2003;47(12):57–63.

[3] Lee DS, Vanrolleghem PA. Monitoring of a sequencing batch reactor using adaptive multiblock principal component analysis. Biotechnol Bioeng 2003;82:489–97.

[4] Dong D, McAvoy TJ. Batch tracking via nonlinear principal component analysis. AIChE J 1996;42(8): 2199–208.

[5] Nomikos P, MacGregor JF. Monitoring batch processes using multiway principal component analysis. AIChE J 1994;40(8):1361–75.

[6] Nomikos P, MacGregor JF. Multivariate SPC charts for monitoring batch processes. Technometryt 1995;37:41–59.

[7] Rännar S, MacGregor JF, Wold S. Adaptive batch monitoring using hierarchical PCA. Chemom Intell Lab Systems 1998;41:73–81.

[8] Kosanovich KA, Dahl KS, Piovoso MM. Improved process understanding using multiway principal component analysis. I&EC 1996;35:138–46.

[9] Tates AA, Louwerse DJ, Smilde AK, Koot GLM, Berndt H. Monitoring a PVC batch process with multivariate statistical process control charts. I&EC 1998;38:4769–76.

[10] Westerhuis JA, Kourti T, Macgregor JF. Comparing alternative approaches for multivariate statistical analysis of batch process data. J Chemometrics 1999;13:397–413.

[11] Gregersen L, Jorgensen SB. Supervision of fed-batch fermentations. Chem Eng J 1999;75:69–76.

[12] Teppola P. Multivariate process monitoring of sequential process data—a chemometric approach, Ph.D. thesis, Lappeenranta University of Technology, Finland, 1999.

[13] Albert S, Kinley RD. Multivariate statistical monitoring of batch processes: an industrial case study of fermentation supervision. Trends Biotechnol 2001;19(2):53–62.

[14] Lennox B, Montague GA, Hiden HG, Kornfeld G, Goulding PR. Process monitoring of an industrial fed-batch fermentation. Biotechnol Bioeng 2001;74(2): 125–35.

[15] Rosen C, Lennox JA. Multivariate and multiscale monitoring of wastewater treatment operation. Water Res 2001;35:3402–10.

[16] Yoo CK, Choi SW, Lee I-B. Disturbance detection and isolation in the activated sludge process. Water Sci Technol 2002;45:217–26.

[17] Yoo CK, Choi SW, Lee I. Dynamic monitoring method for multiscale fault detection and diagnosis in MSPC. I&EC 2002;41:4303–17.

[18] Bicciato S, Bagno A, Solda M, Manfredini R, Bello CD. Fermentation diagnosis by multivariate statistical analysis. Appl Biochem Biotech 2002;102:49–62.

[19] Yoo CK, Lee J-M, Lee I-B. On-line process monitoring with multi-way independent component analysis for continuous and batch process, Technical paper, POSTECH, Korea, 2001.

[20] Lee J-M, Yoo CK, Lee I-B. On-line batch process monitoring using another unfolding method and independent component analysis. J Chem Eng Japan 2003, accepted.

[21] Ündey C, Çinar A. Statistical monitoring of multistage, multiphase batch processes. IEEE Control Systems Mag 2002;10:40–52.

[22] Wold S, Kettanhe N, Friden H, Holmberg A. Modelling and diagnostics of batch processes and analogous kinetic experiments. Chem Intell Lab Sytemss 1998;44: 331–40.

[23] Hyvärinen A. Fast and robust fixed-point algorithms for independent component analysis. IEEE Trans Neural Networks 1999;10:626–34.

[24] Hyvärinen A. Survey on independent component analysis. Neural Comp Surveys 1999;2:94–128.

[25] Hyvärinen A, Oja E. Independent component analysis: algorithms and applications. Neural Networks 2000; 13(4–5):411–30.

[26] Kano M, Tanaka S, Ohno H, Hasebe S, Hashimoto I. Monitoring independent components for fault detection. AIChE J 2002;49(4):969–76.

[27] Lee T. Independent component analysis: theory and applications. Boston: Kluwer Academic Publishers; 1998.

[28] Jackson JE. A user's guide to principal components. USA: Wiley & Sons, INC.; 1991.

[29] Rosen C. A Chemometric approach to process monitoring, control with application to wastewater treatment operation, Ph.D. thesis, Lund University, Sweden, 2001.